



**HAL**  
open science

## Probing the dynamics of quasicrystal growth using synchrotron live imaging

Henri Nguyen-Thi, Joseph Gastaldi, Thomas Schenk, Guillaume Reinhart,  
Nathalie Mangelinck-Noel, Viviana Cristiglio, Bernard Billia, Benjamin  
Grushko, Jürgen Härtwig, Holger Klein, et al.

► **To cite this version:**

Henri Nguyen-Thi, Joseph Gastaldi, Thomas Schenk, Guillaume Reinhart, Nathalie Mangelinck-Noel, et al.. Probing the dynamics of quasicrystal growth using synchrotron live imaging. 2005. hal-00004805v1

**HAL Id: hal-00004805**

**<https://hal.science/hal-00004805v1>**

Preprint submitted on 27 Apr 2005 (v1), last revised 6 Jul 2005 (v2)

**HAL** is a multi-disciplinary open access archive for the deposit and dissemination of scientific research documents, whether they are published or not. The documents may come from teaching and research institutions in France or abroad, or from public or private research centers.

L'archive ouverte pluridisciplinaire **HAL**, est destinée au dépôt et à la diffusion de documents scientifiques de niveau recherche, publiés ou non, émanant des établissements d'enseignement et de recherche français ou étrangers, des laboratoires publics ou privés.

# Probing the dynamics of quasicrystal growth using synchrotron live imaging

H. Nguyen-Thi<sup>1</sup>, J. Gastaldi<sup>2</sup>, T. Schenk<sup>3</sup>, G. Reinhart<sup>1</sup>, N. Manginck-Noel<sup>1</sup>, V. Cristiglio<sup>3</sup>, B. Billia<sup>1</sup>, B. Grushko<sup>4</sup>, J. Härtwig<sup>3</sup>, H. Klein<sup>5</sup>, J. Baruchel<sup>3</sup>

<sup>1</sup>L2MP, UMR CNRS 6137, Université Paul Cézanne Aix-Marseille III, Faculté des Sciences Saint-Jérôme, Case 142, 13397 Marseille Cedex 20, France.

<sup>2</sup>CRMCN-CNRS, Campus Luminy Case 913, 13288 Marseille Cedex 9, France.

<sup>3</sup>ESRF, BP 220, 38043 Grenoble, France.

<sup>4</sup>IFF, Forschungszentrum Juelich GmbH, 52425 Juelich, Germany.

<sup>5</sup>Laboratoire de Cristallographie, CNRS Bât. F, BP 166, 38402 Grenoble Cedex 9, France.

Quasicrystals constitute a distinct class of solids as they differ both from crystals, because they are not periodic, and from glasses, because they have long-range orientation order. The main challenge of quasicrystal physics is certainly to elucidate how the quasiperiodic order can extend up to the centimetre size of the single grains routinely grown nowadays<sup>1-3</sup>. In particular, the dynamics of quasicrystal growth remains an unsolved problem in condensed matter. Here, owing to the incisiveness of synchrotron live imaging, we show evidences that the solidification front of icosahedral AlPdMn quasicrystal is faceted all along the growth which proceeds by the tangential motion of ledges at the solid-melt interface, with a measurable effect of interface kinetics. Increasing the applied solidification rate, the kinetic undercooling becomes large enough for the nucleation and free growth of new faceted grains in the melt. The evolution of these grains is explained in details, which reveals the crucial role of aluminium rejection, both in the poisoning of grain growth and driving fluid flow.

Quasicrystals display long-range orientational order with symmetries (5-fold, 8-fold, ...) incompatible with periodicity, that were previously considered as strictly forbidden. They also exhibit many beneficial specific properties (high hardness, low electric conductivity, low friction coefficient ...) that have motivated engineering efforts to use them as efficient new materials (e.g. for advanced surface coatings, catalysis or

hydrogen-storage). These properties have been more or less successfully related to the peculiar quasicrystal structure. It is therefore critical and timely to deepen the understanding of its dynamical formation during growth from the alloy melt. Whether the formation of the stable quasicrystal structure is constrained by local growth rules<sup>4</sup> or by the establishment of long-range atomic correlation<sup>5</sup> is still undetermined. Because translation symmetry is lacking, it seems unlikely that quasicrystals build up by the attachment of single atoms, thereby generating unit cells and the whole network just like crystals do. However, as icosahedral clusters have been recently identified in quasicrystal-forming liquids<sup>6</sup>, the old idea of growth by the attachment of these clusters at the liquid-solid interface<sup>7</sup> is reviving, this process settling the quasicrystalline structure in a way to be clarified. Besides, the grains displaying facets perpendicular to the symmetry axes (5, 3, 2 for icosahedral quasicrystals), most often observed post mortem, also suggest that quasicrystals may grow by the forward movement of facets resulting from terrace and ledge motion<sup>8,9</sup>. Nonetheless, the difficulty to define quasicrystallographic planes remains by now a serious conceptual obstacle.

In this context, by recording synchrotron radiographs (see section Method) during upward Bridgman solidification we carried out the first live probing of the growth of icosahedral AlPdMn quasicrystals in order to get a clear insight on both the shape of the growing grains and the morphology of the solid-liquid interface. These features were not accessible in the direct observation of rapid solidification at high liquid undercooling<sup>10</sup>, where growth was dendritic. Here, we characterise the dynamical evolution of the quasicrystal grains observed in two solidified AlPdMn samples.

First, *in situ* X-ray imaging unambiguously proves that the quasicrystals do grow with a faceted solid-melt interface (Fig. 1). The radiographs basically show projections along the incident X-ray beam. In Fig. 1a, which corresponds to steady-state growth at a pulling rate of 0.4  $\mu\text{m/s}$ , two grains are growing simultaneously upwards, and the interface between the liquid and these grains shows a cusp at the level of the grain boundary. From the outline of the solid – melt interface, facets and facet edges can be identified on grain 1 and grain 2, which are dodecahedra extending in the direction of pulling (the dodecahedron superposed on Fig. 1a gives the orientation of grain 2). Then, as soon as the applied pulling velocity is increased to 3.6  $\mu\text{m/s}$ , a solidification transient takes place in which the growth velocity (Fig. 2) and grain shape progressively adapt. After about 600s, the net result (Fig. 1b) is double. On the one hand, the solidification front has globally

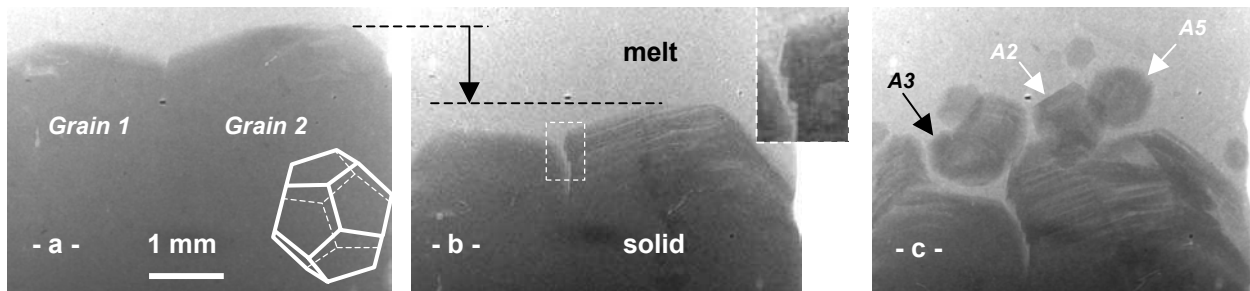


**Figure 1** Images recorded by *in situ* and real-time X-ray radiography of AlPdMn quasicrystals growing from their melt : (a) at the end of a growth sequence achieved with a pulling rate  $V = 0.4 \mu\text{m/s}$ , (b) and (c) during the growth sequence at  $V = 3.6 \mu\text{m/s}$ . The front recoil due to the increase of the applied pulling velocity is shown by the downward arrow in Fig. 1b. The dashed lines in the insert of Fig. 1b and in Fig. 1c are to guide the eyes, and allow orientation by referring to the dodecahedron superposed on Fig. 1a.

receded to a lower temperature, and the growth rate reached the new pulling velocity. On the other hand, the cusp has evolved into a wide and deep liquid groove and while advancing the facets have developed evidences of ledge growth (tangential motion of macrosteps, or bunches of macrosteps), namely the striations running parallel to the solid – liquid interface and the notches neatly visible on the left side of grain 2 (see insert in Fig. 1b, and Fig. 1c). Models based on normal growth with “thick” diffuse interface region<sup>5,7</sup> are not suited to describe ledge growth. The striations and notches are very likely resulting from the repeated kinetic instability of the facets leading to the development of skeletal shapes, as recognised in solution growth<sup>11</sup>. Accordingly, because of locally higher undercooling and solid – liquid interface roughness, ledges are generated during growth from the melt at facet edges and vertices. Then, the tangential motion of these ledges scraps the chemical species rejected in the melt upon solidification, mostly aluminium, down over the facets. This process has a self-poisoning effect on ledge spreading, eventually until cessation stopping the facet normal advance. The observed striations would thus delineate arrests of ledges, that merely appear as notches when viewed from the side.

Furthermore, the front recoil caused by the increase of the pulling velocity, which is materialised by the downward arrow in Fig. 1b, indicates that the attachment of the building elements in the melt to the quasicrystal solidification front is uneasy, and thus needs significant departure from thermodynamic equilibrium to drive the growth process. As ledge limited growth is characterised by linear kinetics<sup>12</sup>, assuming identical solutal recoil<sup>13</sup> the velocity jump  $\Delta V$  and temperature shift  $\Delta T$  between Fig. 1a and Fig. 1b can be related by the relation  $\Delta V = -\mu\Delta T$  with  $\mu$  the kinetic coefficient. Using the experimental values  $\Delta V = 3.2 \mu\text{m/s}$  and  $\Delta T = -1 \text{ K}$  gives  $\mu = 0.9 \mu\text{m}\cdot\text{s}^{-1}\cdot\text{K}^{-1}$ . As far as we are aware, this method for the first time allows to directly derive a realistic lower estimate of the kinetic coefficient  $\mu$ . This value is two orders of magnitude larger than the value derived by Dong et al.<sup>14</sup> using the Avrami approach of isothermal phase transformation. As the Avrami exponent was defined for the late stage of the transformation only, this discrepancy can be attributed to the slowing down of the process as, on the one hand, grain growth was continuously poisoned by the aluminium rejected upon solidification causing concomitant reduction of the effective undercooling, and, on the other hand, grain impingement developed, characterised by strong overlapping of the diffusion fields of the various grains. Actually, live observation shows that quasicrystal growth kinetics is not so sluggish as admitted but rather comparable to

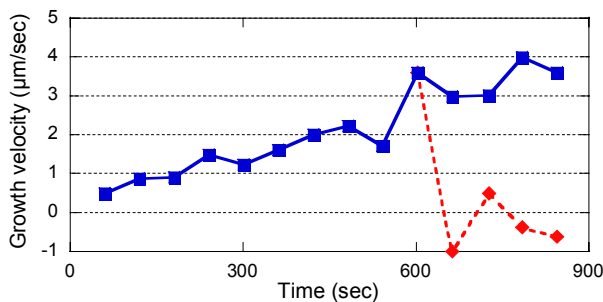


**Figure 2** Evolution of the growth velocity of grain 1 in the solidification transient following the abrupt increase of the applied pulling rate from  $V = 0.4$  to  $V = 3.6 \mu\text{m/s}$ . The dashed curve ( $\blacklozenge$ ) shows the rapid blockage of the growth of the right part of grain 1 by a newly nucleated grain, which is visible in Fig. 1c.

the ledge growth kinetics of semiconductors, intermetallics and oxides ( $\mu = 0.826 \mu\text{m}\cdot\text{s}^{-1}\cdot\text{K}^{-1}$  was found for  $\text{Bi}_4\text{Ge}_3\text{O}_{12}$ <sup>15</sup>), definitely much slower than the solidification kinetics of pure metals.

Second, 60 sec after Fig. 1b small faceted quasicrystals nucleate and grow freely in the melt just ahead of grains 1 and 2 (Fig. 1c). By their growth these grains provoke solutal blockage<sup>16</sup> due to the mutual impediment of the evacuation of the rejected aluminium, which thus accumulates in the narrow spaces between the grains. This process effectively begins with the screening of grains 1 and 2 (Fig. 2), like in the regular columnar-to-equiaxed transition commonly observed in casting<sup>16</sup>. It is worth noticing the black contrast lines decorating the grains in the radiographs (Fig. 3a-c). Indeed, these lines are revealing the segregation of the densest and thus most X-ray absorbing component, namely palladium, at grain edges and vertices. Besides, the geometry of the contrast lines in practice enable the determination of grain orientation (Fig. 3d,e), as done for grain 2 in Fig. 1 at an early stage of its development. This method is somewhat similar to the one used to orient dendritic icosahedral- $\text{AlMn}$  grains from optical metallographs<sup>17</sup>. The radiographs show that the new faceted grains are dodecahedral polyhedra often oriented with either a twofold (e.g. A2 in Fig. 1c and Fig. 3b) or fivefold axis (e.g. A5 in Fig. 1c and Fig. 3a) along the incident X-ray beam. A threefold axis is more rarely observed (e.g. A3 in Fig. 1c).

The velocity of each facet or edge making the outline of a free grain can be measured along the normal to its trace on the radiographs (Fig. 4). It follows that all these velocities initially increase with time and ultimately fall down when a facet and a neighbour grain are growing towards each other. Then, facet growth and grain growth progressively interfere due to the increasing overlap of the diffusion fields, and the facet velocity reaches zero when impingement occurs. At short times, the growth of the new grain is free but not isotropic, which is most obvious for the edges propagating upwards and downwards (arrows 1 and 6 respectively). We interpret this asymmetry as the very signature of thermosolutal convection, well-known for dendrites<sup>18</sup>. Indeed, the rejection of both aluminium and latent heat renders the melt surrounding the solid grain lighter, thus creating a driving force for growth-induced natural convection.

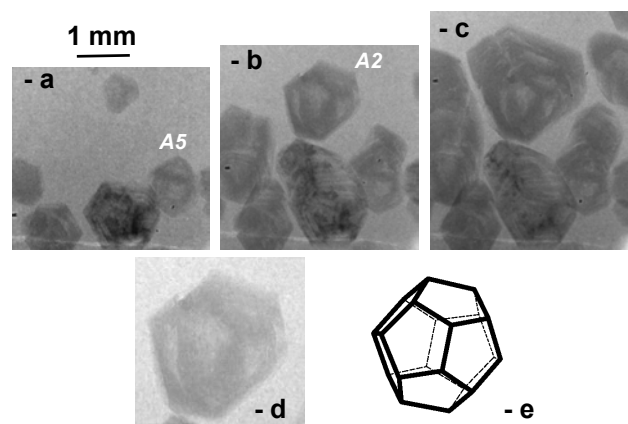


**Figure 3** Typical evolution of a free grain after nucleation in the melt, showing progressive blockage by neighbours : - a) 180 sec, - b) 421 sec, - c) 843 sec after nucleation. Pulling rate  $V = 3.6 \mu\text{m/s}$ . Grain orientation deduced from radiography contrast (d) is shown by projected dodecahedron (e).

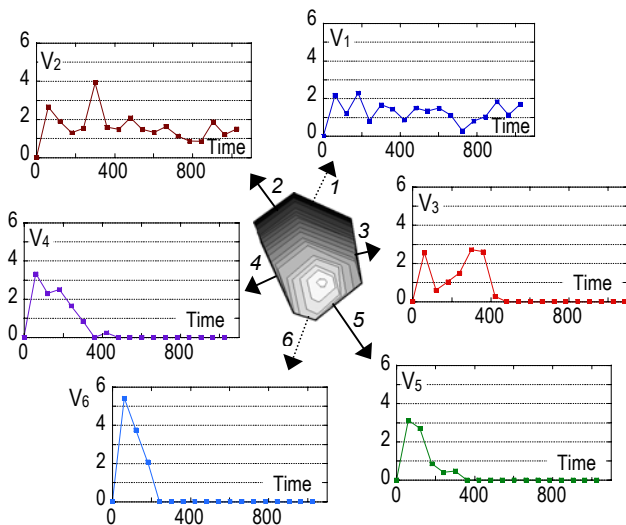


**Figure 4** Variation with time (in sec) of the velocity (in  $\mu\text{m}/\text{sec}$ ) of the facets (arrows 2 – 5, velocities  $V_2 - V_5$ ) and edges (arrows 1 and 6, velocities  $V_1$  and  $V_6$ ) making the outline of the highest grain in Fig. 3a. The origin of time is set at grain nucleation, 540 s after applying the pulling rate  $V = 3.6 \mu\text{m}/\text{s}$ . Notice the high asymmetry of the growth velocities of edge 1 and edge 6.

For the downward - growing edge, this buoyancy - driven convection sweeps the surrounding fluid away upwards, and brings much undercooled melt in contact with this edge, which causes it to grow faster. For the upward-growing edge, the low-undercooling fluid enveloping the grain flows upwards into the path of the edge which causes it to propagate more slowly. The dodecahedron shape is preserved as long as grain growth is free, i.e. not suffering neighbour interaction altering the contour. Indeed, in the process of grain impingement, the facets facing each other undergo progressive smoothening that gives way to curved boundaries. Meanwhile, the facets seeing open melt ahead, that generally grow at a small angle to the pulling direction, conversely persist and continue to advance. This stage, which may even reach a steady-state as indicated by the plateaux in the velocities of facet 1 and facet 2, results in grain elongation (Fig. 3b,c).

The mere fact that the nucleation of new grains does not occur during the growth sequence at  $V = 0.4 \mu\text{m}/\text{s}$  but only after the increase to  $V = 3.6 \mu\text{m}/\text{s}$  brings out fundamental information. Namely, it is because the kinetic undercooling needed for quasicrystal growth has exceeded the critical nucleation undercooling that the birth of new grains is enabled in the melt just above grains 1 and 2. For the sound discussion of nucleation and growth kinetics, the building units and their supersaturation in the solution need to be identified. Due to the topological similarity between the local structural order of icosahedral AlPdMn and the icosahedral clusters in the melt<sup>6,19</sup>, a very low resistance of icosahedral quasicrystals to nucleation is expected. This suggests that the new grains grow from such clusters so that the nature of quasicrystal nucleation, which remains presently uncertain, may be blurred : heterogeneous because on solid embryos, homogeneous because these embryos are icosahedral clusters structurally self-embedded in the melt and not added refining particles. However, a critical nucleation radius comparable to the icosahedral cluster size for  $\Delta T_k = 1^\circ\text{C}$  implies an extremely small solid – liquid interface energy, so

that atom – sharing polyclusters formed by individual clusters linked together<sup>6,20</sup> in the melt seems better candidates for the nucleation embryos. Besides, a catalytic effect of heterogeneous nucleation, in particular on the graphite crucible walls, seems unlikely because it is hardly conceivable that the structure of the heterogeneity surface better matches the quasicrystal - melt interface structure than the polycluster surface.

Using synchrotron live imaging to probe *in situ* and in real-time the dynamics of icosahedral AlPdMn quasicrystal growth from the melt, we unambiguously establish the faceted character of grain growth. This process is driven by a ledge spreading mechanism. From the analysis of the solid – melt interface undercooling, a realistic estimate of the kinetic coefficient is for the first time deduced, much larger than the values available in the literature. We must also conclude that, rather than by local heat flow, the growth of quasicrystals is controlled by interface kinetics, and aluminium diffusion as further evidenced in a detailed analysis of the free growth of new AlPdMn quasicrystals.

## Methods

The experiments were performed by *in situ* and real time synchrotron X-ray radiography at the ID 19 beamline of the European Synchrotron Radiation Facility (ESRF) in Grenoble, France. They consisted in recording all along growth absorption and phase contrast images delivered in monochromatic mode by the highly coherent X-ray beam<sup>21</sup> after crossing a sample solidifying between two graphite foils. The images were recorded either continuously with a CCD camera or at intervals on High Resolution films or in live<sup>22</sup>. The Bridgman directional solidification set-up allows the independent control of both the pulling velocity and the temperature gradient<sup>23</sup>. Two 700  $\mu\text{m}$ -thick sheets were made by grinding polygrained rods of AlPdMn alloy prepared at the composition  $\text{Al}_{72.4}\text{Pd}_{20.5}\text{Mn}_{7.1}$  known to give directly the icosahedral quasicrystal phase<sup>1</sup>. These sheets were first melted, and then solidified at various pulling velocities (0.4 – 3.6  $\mu\text{m}/\text{s}$ ) under the same temperature gradient of 35 K/cm. Quasicrystallinity was checked by recording Laue patterns and Energy-Dispersive Spectra.

1. Boudard, M., Bourgeat-Lami, E., de Boissieu, M., Janot, C., Durand-Charre, M., Klein H., Audier M. & Hennion B. Production and characterization of single quasicrystals of the Al-Pd-Mn icosahedral phase. *Phil. Mag. Lett.* **71**, 11-19 (1995).
2. Yokoyama, Y., Note, R., Kimura, A., Inoue, A., Fukaura, K. & Sunada, H. Preparation of decagonal Al-Ni-Co single quasicrystal by Czochralski method. *Mat. Trans. JIM* **38**, 943-949 (1997).
3. Langsdorf, A. & Assmus, W. Growth of large single grains of the icosahedral quasicrystal ZnMgY. *J. Crystal Growth* **192**, 152-156 (1998).
4. Dmitrienko, V. E., Astaf'ev, S. B. & Kléman M. Monte Carlo simulations of icosahedral quasicrystal growth and melting. *Phys. Rev. B* **59**, 286-293 (1999).
5. Henley, C. L. Quasicrystal order, its origins and its consequences: a survey of current models. *Comm. Cond. Matt. Phys.* **13**, 59-117 (1987).
6. Simonet, V., Hippert F., Audier, M. & Bellisent, R. Local order in liquids forming quasicrystals and approximant phases. *Phys. Rev. B* **65**, 024203 (2001).
7. Elser, V., in *Extended Icosahedral Structures* (eds Jaric, M. V. & Gratias, D.) Vol. 3, 105-136 (Academic Press, Boston, 1989).
8. Beeli, C. & Nissen, H. U. Growth morphology of icosahedral Al-Mn-Pd single quasicrystals. *Phil. Mag. B* **68**, 487-512 (1993).
9. Toner, J., Growth and kinetic roughening of quasicrystals and other incommensurate systems. *Phys. Rev. Lett.* **59**, 930-933 (1990).
10. Schroers, J., Holland-Moritz, D., Herlach D. M. & Urban, K. Growth kinetics of quasicrystalline and polytetrahedral phases of Al-Pd-Mn, Al-Co and Al-Fe from the undercooled melt. *Phys. Rev. B* **61**, 14500- 14506 (2000).

11. Chernov, A. A. Stability of faceted shapes. *J. Crystal Growth* **24/25**, 11-31 (1974).
12. Tiller, W. A. *The science of crystallization : Microscopic interfacial phenomena*. Ch. II (Cambridge Univ. Press, Cambridge, UK, 1991).
13. Caroli, B., Caroli, C. & Ramirez-Piscina, L. Initial front transients in directional solidification of dilute alloys. *J. Crystal Growth* **132**, 377-388 (1993).
14. Dong, C., Dubois, J.M., de Boissieu, M., Boudard, M. & Janot, C. Growth of stable Al-Pd-Mn icosahedral phase. *J. Mater. Res.* **6**, 2637-2645 (1991).
15. Golyshev, V.D., Gonik, M.A. & Tsvetovsky, V.B. In situ measurement of interface supercooling during melt crystal growth. *J. Crystal Growth* **237-239**, 735-739 (2002).
16. Martorano, M.A., Beckermann, C. & Gandin, Ch.-A. A solutal interaction mechanism for the columnar-to-equiaxed transition in alloy solidification. *Metall. Mater. Trans. A* **34**, 1657-1674 (2003).
17. Schaefer, R.J., Bendersky, L.A., Schechtman, D., Boettinger, W.J. & Biancaniello, F.S. Icosahedral and decagonal phase formation in Al-Mn alloys. *Met. Trans. A* **17**, 2117-2125 (1986).
18. Tirmizi, S. H. & Gill, W. N. Effect of natural convection on growth velocity and morphology of dendritic ice crystals. *J. Crystal Growth* **85**, 488-502 (1987).
19. Tanaka, H. Roles of local icosahedral chemical ordering in glass and quasicrystal formation in metallic glass formers. *J. Phys.: Condens. Matter* **15**, L491-L498 (2003).
20. Rossi, G., Rapallo, A., Mottet, C., Fortunelli, A., Baletto, F. & Ferrando, R. Magic polyicosahedral core-shell clusters, *Phys. Rev. Lett.* **93**, 105503 (2004).
21. Cloetens, P., Barrett, R., Baruchel, J., Guigay, J.P. & Schlenker, M. Phase objects in synchrotron radiation hard X-ray imaging, *J. Phys. D* **29**, 133-146 (1996).
22. Labiche, J.C., Segura-Puchades, J., Van Brussel, D. & Moy, J.P. FRELON Camera: Fast REadout LOW Noise, *ESRF Newslett.* **25**, 41-45 (1996).
23. Nguyen Thi, H., Jamgotchian, H., Gastaldi, J., Härtwig, J., Schenk, T., Klein, H., Billia, B., Baruchel, J. & Dabo, Y. Preliminary in situ and real time study of directional solidification of metallic alloys by X-ray imaging techniques, *J. Phys. D* **36**, A83-A86 (2003).

**Acknowledgements** The authors express their gratitude to T. Bactivelane, R. Chagnon for technical assistance in the preparation of the experiments, and completion at ESRF. They also thank M. Kleman, V. Dmitrienko and M. de Boissieu for fruitful discussions.

**Correspondence** should be addressed to H.N.T. (henri.nguyen-thi@L2MP.fr).